Available online at www.sciencedirect.com
SCIENCE DIRECT
Physics and Chemistry of the Earth 31 (2006) 365–377
PHYSICS and CHEMISTRY of the EARTH
www.elsevier.com/locate/pce

# Precursory phenomena associated with the 1999 Chi-Chi earthquake in Taiwan as identified under the iSTEP program

Yi-Ben Tsai [a], Jann-Yenq Liu [b,c,*], Kuo-Fong Ma [a], Horng-Yuan Yen [a], Kun-Shan Chen [c], Yuh-Ing Chen [d], Chien-Ping Lee [a]

[a] *Institute of Geophysics, National Central University, Chung-Li 320, Taiwan*
[b] *Institute of Space Science, National Central University, Chung-Li 320, Taiwan*
[c] *Center for Space and Remote Sensing Research, National Central University, Chung-Li 320, Taiwan*
[d] *Institute of Statistics, National Central University, Chung-Li 320, Taiwan*

Accepted 6 February 2006

**Abstract**

This paper presents a brief summary of several types of precursors in the lithosphere, atmosphere and ionosphere that have been positively identified in relation to the 20 September 1999 $M_w$ 7.6 Chi-Chi earthquake and its aftershocks under the iSTEP Program.


*Keywords:* iSTEP; Chi-Chi earthquake; P-wave; DInSAR; Geomagnetic; Atmospheric; Ionospheric; Aftershock

## 1. Introduction

An $M_w$ 7.6 earthquake struck central Taiwan with its epicenter near the small town of Chi-Chi at 01:47 LT (local time) on 21 September 1999. It caused loss of more than 2500 lives and collapse of more than 100,000 residential housing units. A program on integrated Search for Taiwan Earthquake Precursors (iSTEP) has been carried out since 1 April 2002. In this paper we summarize several types of positively identified precursory phenomena along with statistical analyses, including seismological variations, geomagnetic field changes, ground surface deformation, and ionospheric variations associated with the Chi-Chi earthquake and its aftershocks.

## 2. Observations and statistical analysis

Through seismological, geomagnetic, surface deformation, and ionospheric observations, we have identified several types of possible precursory phenomena up to the time of the Chi-Chi earthquake by different methods. Fig. 1 synthesizes the results of these observations in a common time frame.

### 2.1. Increase of P-wave travel-time residuals

P-wave travel-time residuals determined as a by-product of earthquake location by the Taiwan Central Weather Bureau Seismic Network were used to study the variations of P-wave velocity structure in the crust near the Chi-Chi earthquake focal area (Lee and Tsai, 2004). The results obtained by using seismic data from 1991 to 2002 show that the mean P-wave travel-time residuals increased at the stations immediately west of the Chelungpu fault about six years before the Chi-Chi earthquake. Fig. 2 shows the variations of P-wave residuals at station NSY near northern part of the Chelungpu fault from 1991 to 2002. The

* Corresponding author. Address: Institute of Space Science, National Central University, Chung-Li 320, Taiwan. Tel.: +886 3 422 8374; fax: +886 3 422 4394.
*E-mail address:* jyliu@jupiter.ss.ncu.edu.tw (J.-Y. Liu).

1474-7065/$ - see front matter © 2006 Elsevier Ltd. All rights reserved.
doi:10.1016/j.pce.2006.02.035

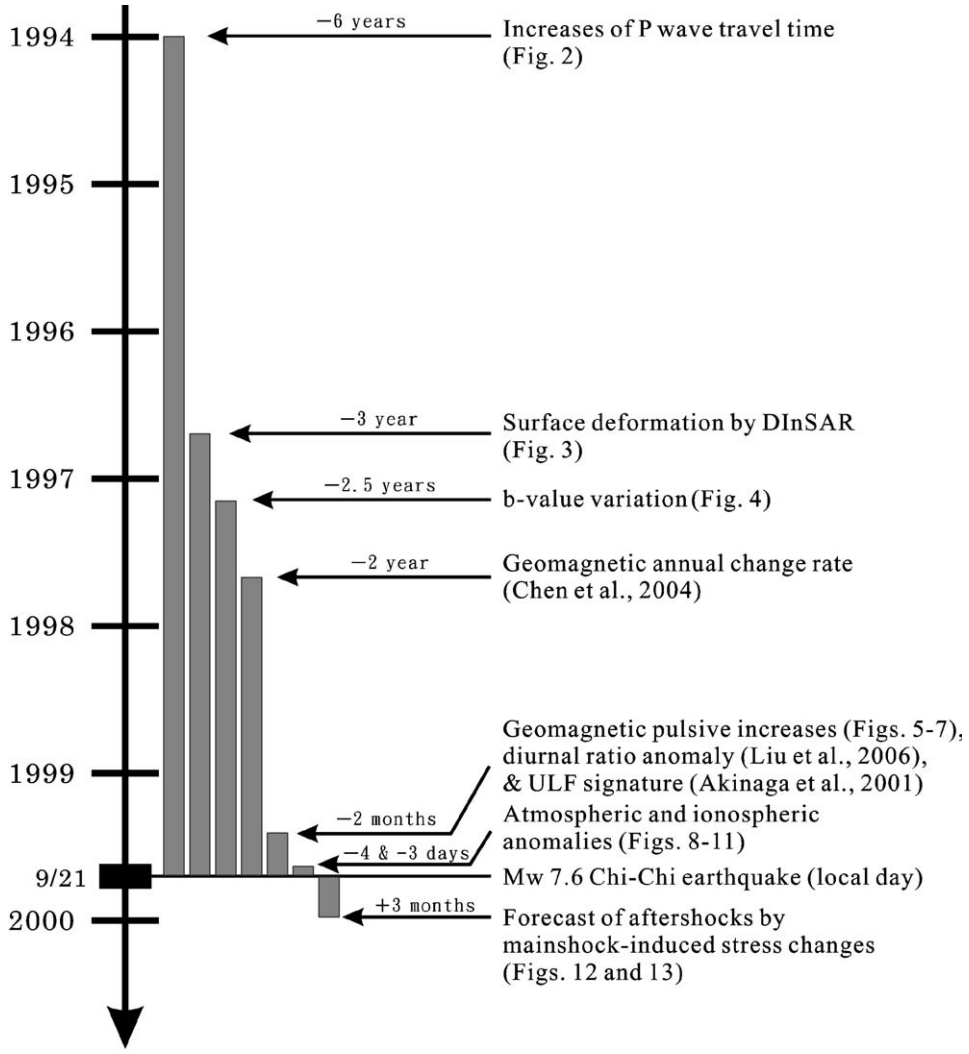


Fig. 1. Time lines of the precursors of the 1999 Chi-Chi, Taiwan earthquake, as identified under the iSTEP Program.

contour map below shows that most P waves passing through the anomalous zone east of the Chelungpu fault produced positive residuals from 1994 to the Chi-Chi earthquake. The anomalous zone is bounded by stations within 40 km east the Chelungpu fault. It implies that P-wave velocity began to decrease east of the Chelungpu fault in 1994, as a six-year precursor, possibly due to dilatancy or development of cracks in the crust (Nur, 1972).

### 2.2. Surface deformation before the Chi-Chi earthquake by DInSAR

Carefully chosen ERS-2 radar images were used to identify possible precursory surface deformation in the areas near the Chelungpu fault before the Chi-Chi earthquake. It was found that surface deformation began at least three years before the Chi-Chi earthquake in the areas immediately to the west of the northern segment of the Chelungpu fault where clear co-seismic surface deformation patterns were observed. Fig. 3 compares the DInSAR interferograms of the areas near the Chelungpu fault for three consecutive years before and one year after the earthquake.

### 2.3. Seismicity changes

In order to investigate possible precursory seismicity changes preceding the Chi-Chi earthquake, we calculated the *b*-value of the magnitude–frequency distribution (Gutenberg and Richter, 1944) in the three regions over the north, central and south parts of the Chelungpu fault (Fig. 4a). Based on complete recording of $M \geqslant 2.0$ earthquakes within 40 km in depth, temporal variations of the *b*-value from 1994/1/1 to 1999/8/31 in each of the three regions are presented in Fig. 4b. The *b* values were computed using a 100-event window sliding by 10 events. It is found that the highest *b*-value in region A appears in early 1997 and the *b*-value in region B reaches its peak in late 1997. Therefore, the *b*-value anomalies in regions A and B are a possible precursor of the Chi-Chi earthquake. Finally, although there are relatively high *b*-values in

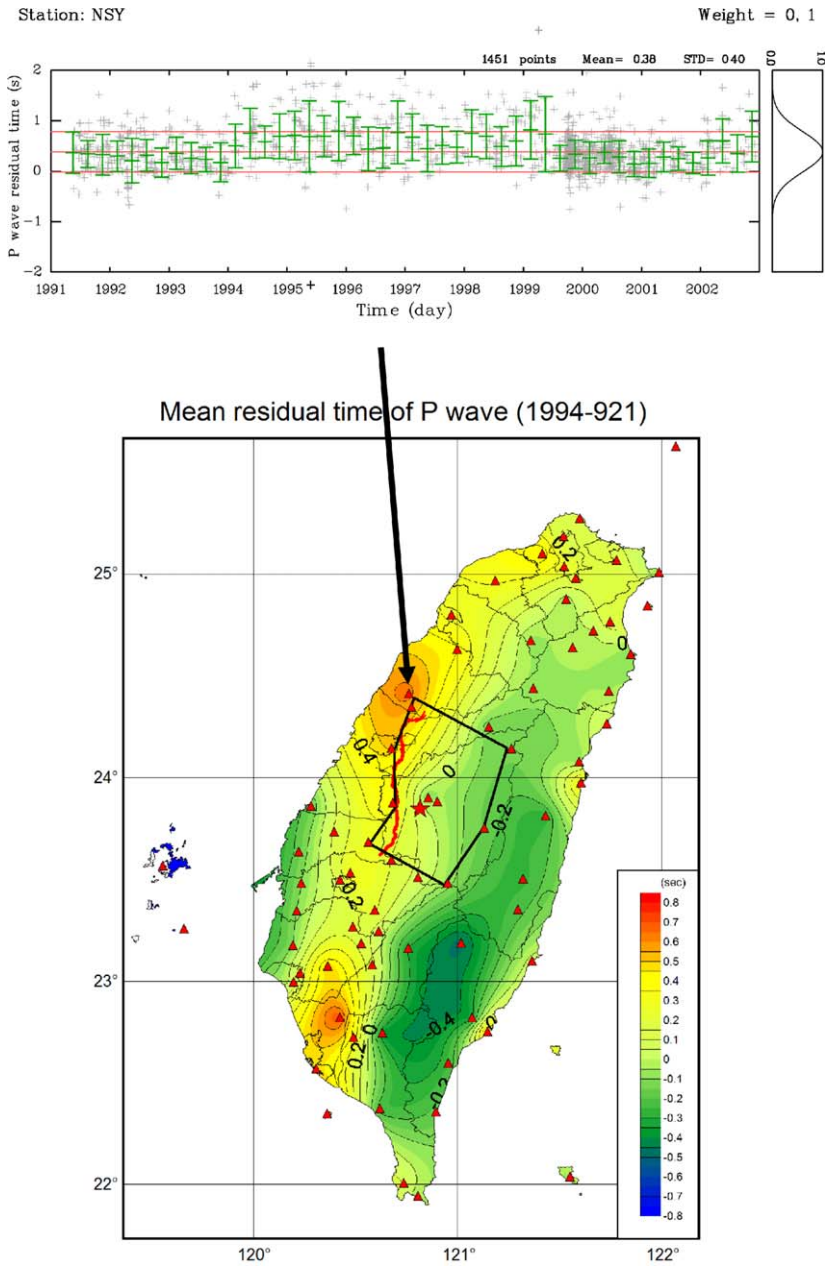


Fig. 2. Top: The variations of P-wave travel-time residuals at station NSY. The phase-reading weights of P-wave travel-time residuals used are 0 and 1. Red lines show the mean and standard deviations of P-wave travel-time residuals from 1991 to 2003. Green lines show the mean and standard deviations of P-wave travel-time residuals in three-month intervals. Bottom: The contour map shows the mean P-wave travel-time residuals from 1994 to the Chi-Chi earthquake. (For interpretation of the references to colour in this figure legend, the reader is referred to the web version of this article.)

region C during 1997, the $b$-value dramatically decreases to 0.65 after the $M$ 6.2 Ruey-Li earthquake on 1998/7/1. Hence, the $b$-value anomaly in region C is likely contaminated by aftershocks of the Ruey-Li earthquake.

To study the spatial variations of the $b$-value over the study region, we further apply the dense-gridding technique (Wiemer and Katsumata, 1999) which takes overlapping grids centered at nodes 5 km apart with 20 km in radius. The primary objective is to find where the significant $b$-value changes occur before the Chi-Chi earthquake. Suppose that, in one grid, there are $n_1$ and $n_2$ earthquakes with magnitudes $\{M_{11}, M_{12}, \ldots, M_{1n_1}\}$ and $\{M_{11}, M_{12}, \ldots, M_{1n_2}\}$ occurred in 1994–1995 and 1997, respectively. Suppose that the associated average magnitudes are $\overline{M_1}$ and $\overline{M_2}$, respectively, and the corresponding $b$-values are $b_1$ and $b_2$, respectively. The standardized $b$-value change is then given by

$$Z_b = (b_2 - b_1)/\{V(b_1) + V(b_2)\}^{1/2},$$

where $V(b_i) = 5.29(b_i)^4 \sum_{j=1}^{n_i} (M_{ij} - \overline{M_i})^2/[n_i(n_i - 1)]$ (Shi and Bolt, 1982) is the estimated variance of $b_i$, $i = 1, 2$. Therefore, a grid is claimed to have an anomalous change, at an approximate significance level of 0.10, if the associated $Z$ value is greater than 1.282 or less than $-1.282$.

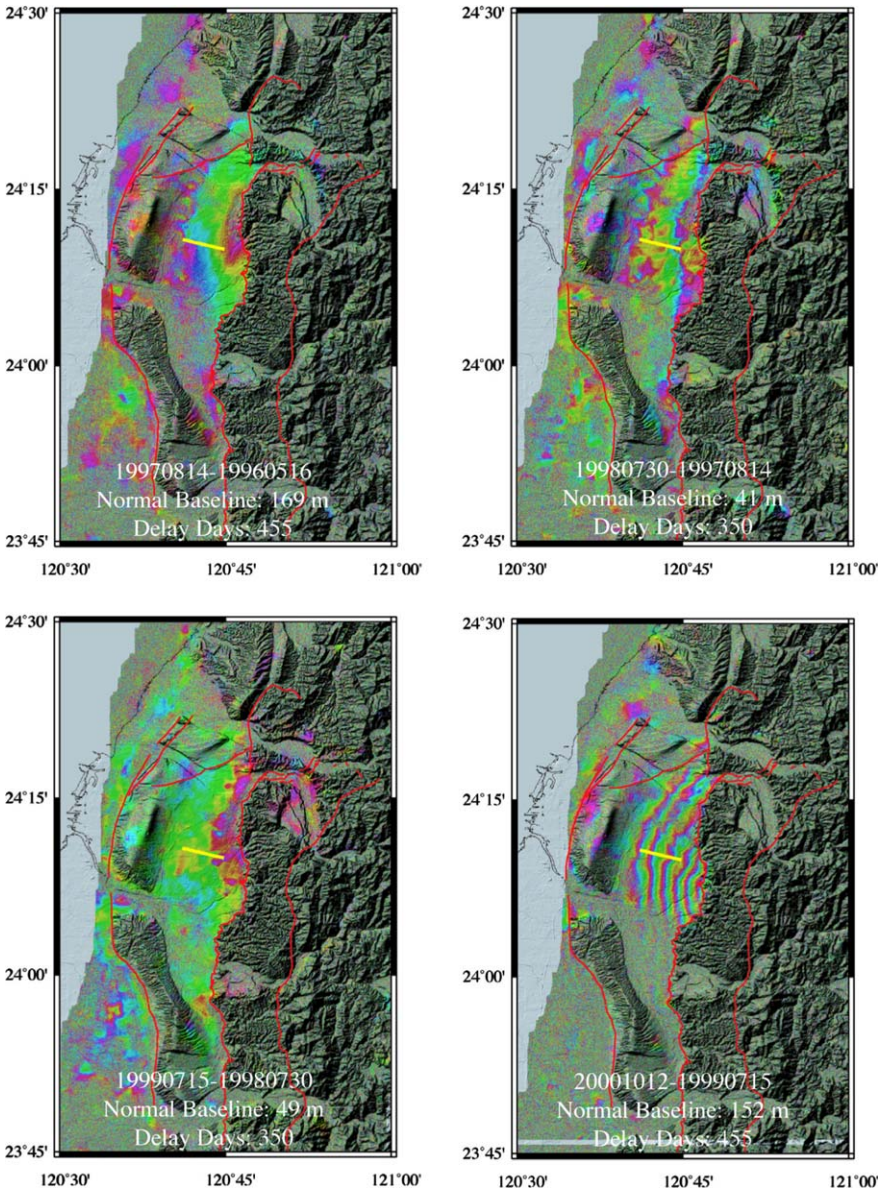


Fig. 3. Radar interferograms of the Taichung basin. Upper left hand side shows the pattern before the Chi-Chi earthquake between 1996/05/16 and 1997/08/14. Upper right hand side shows the pattern before the earthquake between 1997/08/14 and 1998/07/30. Lower left hand side shows the pattern before the earthquake between 1998/07/30 and 1999/07/15. Lower right hand side shows the pattern after the earthquake between 1999/07/15 and 2000/10/12.

The spatial variations of the $Z$ values in Fig. 4c suggest a significant $b$-value increase to the west of northern Chelungpu fault together with a significant $b$-value decrease to the east of central Chelungpu fault just north of the Chi-Chi epicenter. Moreover, in region C, the increase and decrease of $b$-values are significant in the southwest and east, respectively, of the Ruey-Li epicenter. Again, such a seismicity anomaly indicates a possible precursor of the Ruey-Li earthquake.

### 2.4. Geomagnetic fluctuations during the 1999 Chi-Chi earthquake in Taiwan

Fluctuations in geomagnetic field associated with changes in tectonic stress in Taiwan were observed as part of the earthquake prediction research program. An island-wide geomagnetic network of eight stations equipped with continuous recording systems was completed in 1988 by the Institute of Earth Sciences, Academia Sinica (Fig. 5). A proton precession magnetometer (Geometrics Model G-856) with a 0.1 nT sensitivity and continuous recording system was deployed at each station. All stations were located in areas of high seismicity or crustal activity, except for the Lunping (LP) station. The LP station is located in a seismically quiet area in northern Taiwan and is considered as a reference station. In other words, we assume that there is no stress effect on geomagnetic intensity at this reference station. The Liyutan (LY) and the Tsengwen (TW) stations are located in western Taiwan. The other five stations, Neicheng (NC), Hualien (HL), Yuli (YL), Taitung (TT)

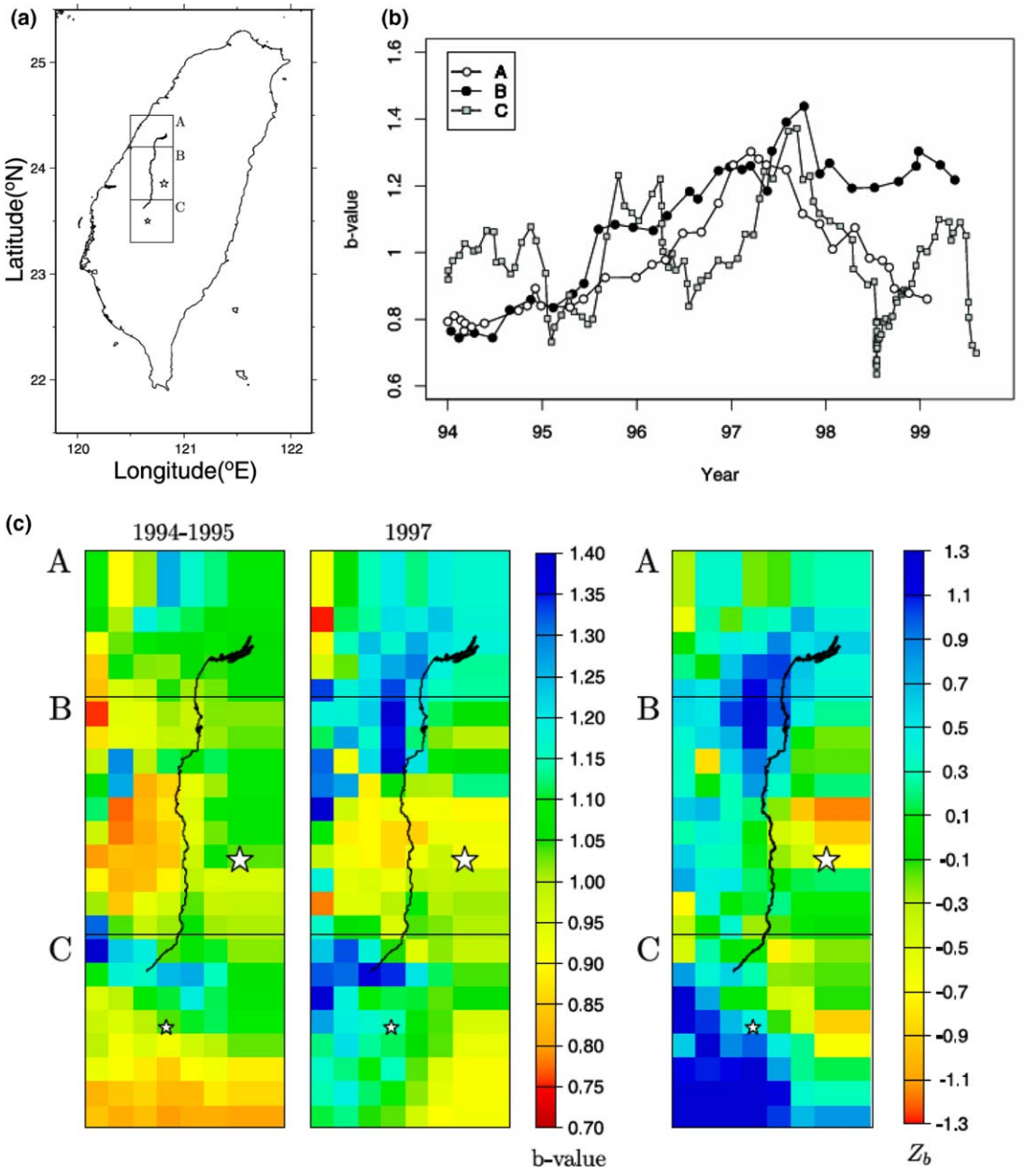


Fig. 4. (a) The three regions along the Chelungpu fault. The large star shows the epicenter of the Chi-Chi earthquake and the small star is for the Ruey-Li earthquake. (b) The temporal variations of the *b*-value. The *b*-values in each of the three regions are computed based on 100-event time windows which are sliding by 10 events. (c) The spatial variations of the *b*-value. The left two figures show the *b*-values in 1994–1995 and 1997, respectively. The right figure is the standardized difference between the *b*-value in 1997 and that in 1994–1995.

and Hengchun (HC), are distributed over eastern and southern Taiwan. The sampling rate at the LP station is at 5-min intervals, while the other stations are at 10-min intervals. We visit the stations routinely every two months to collect data and to maintain the instruments.

After the Chi-Chi earthquake, geomagnetic data recorded by the network were analyzed. Fig. 6 shows the total geomagnetic intensity at the reference station (LP) between mid-August and November 1999. Two magnetic storms were observed at about two days after the Chi-Chi earthquake and at about the time of occurrence of the Chia-Yi earthquake, respectively. The LP station is located about 130 km from the epicenter of the Chi-Chi earthquake and 185 km from the Chia-Yi earthquake. It was concluded that the total geomagnetic intensity at the reference station (LP) did not show any disturbance before or at the time of either the Chi-Chi earthquake or the Chia-Yi earthquake since the station is too far away from the earthquakes.

The differences in geomagnetic total intensity between the LY station and the reference station, the LP station, between mid-August and November 1999 were calculated and plotted as shown in Fig. 7. This figure revealed that the differences fluctuated significantly. The largest

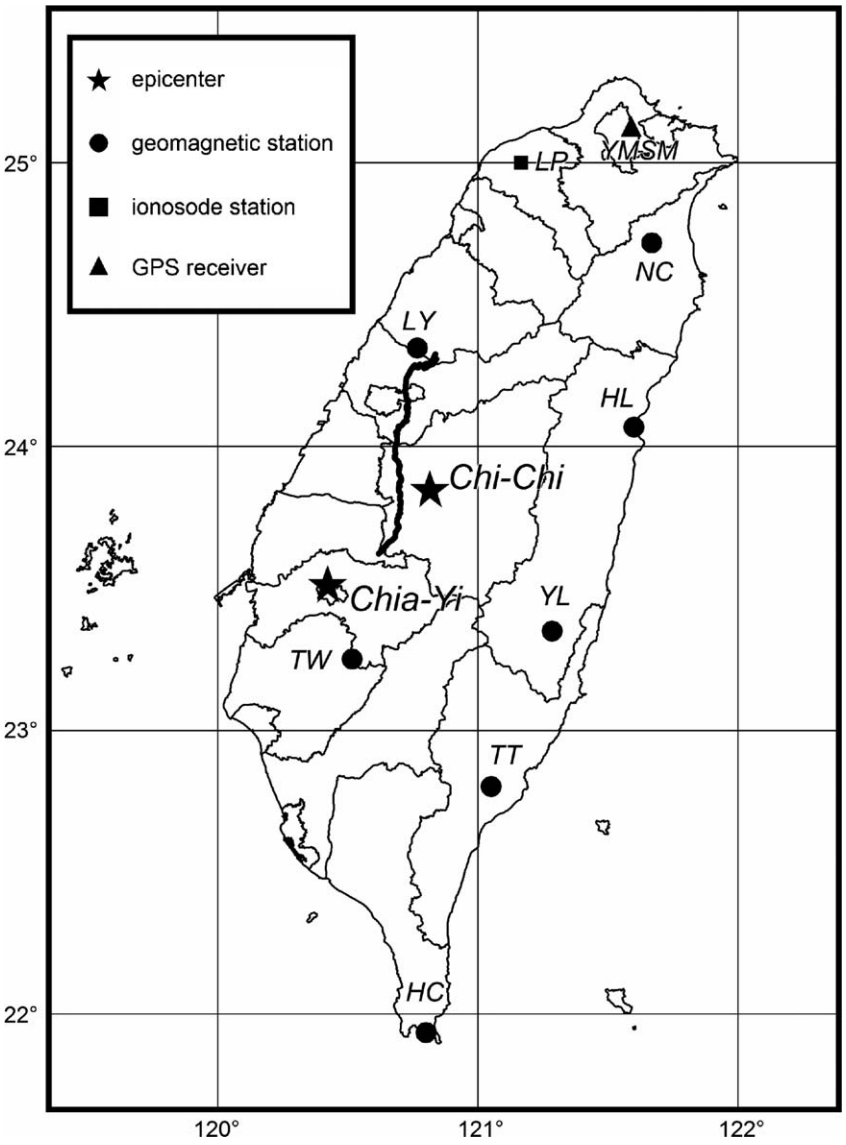


Fig. 5. The locations of geomagnetic stations are denoted by solid squares (old reference station), solid circles (the renovated existing network stations), and solid triangles (the new network stations). All stations are located in seismically active areas except for the Lunping (LP) station that is considered to be a reference station. Solid stars denote the epicenters of the Chi-Chi and Chia-Yi earthquakes. The line in central Taiwan indicates the extent of surface ruptures along the Chelungpu fault.

amplitude reached up to 200 nTs. These signals of disturbance were observed before the Chi-Chi earthquake and continued thereafter. Their amplitudes gradually weakened, and the disturbance levels reduced to that of a quiet period almost right after the $M$ 6.2 Chia-Yi earthquake that occurred near the southern end of the Chelungpu fault (as shown in Fig. 7) on 22 October 1999. These geomagnetic disturbances with highly anomalous amplitudes associated with the Chi-Chi and Chia-Yi earthquakes appear to have been the result of the accumulation and release of crustal stress that subsequently led to severe fault ruptures at the time of the earthquakes.

This phenomenon is quite consistent with the ULF anomalies observed previously by Akinaga et al. (2001), as well as the diurnal geomagnetic anomalies observed by Liu et al. (2006).

### 2.5. Atmospheric and ionospheric anomalies

Electromagnetic phenomena possibly associated with seismic activities have been extensively reported in literatures (e.g. Hayakawa and Fujinawa, 1994; Hayakawa, 1999, 2000; Hayakawa and Molchanov, 2002).

It has been known that the atmospheric conductivity could be changed during the earthquake preparation period. A network of lightning detectors in Taiwan has been continuously monitoring the occurrences of lightning due to cloud to ground (C–G) discharges. Fig. 8 illustrates the lightning occurrence 15 days before and after the Chi-Chi earthquake, respectively. It is found that the lightning occurrence significantly increases on 17 September 1999, which is 4 days before the earthquake. Fig. 9 further shows that the C–G discharges on 17 September 1999

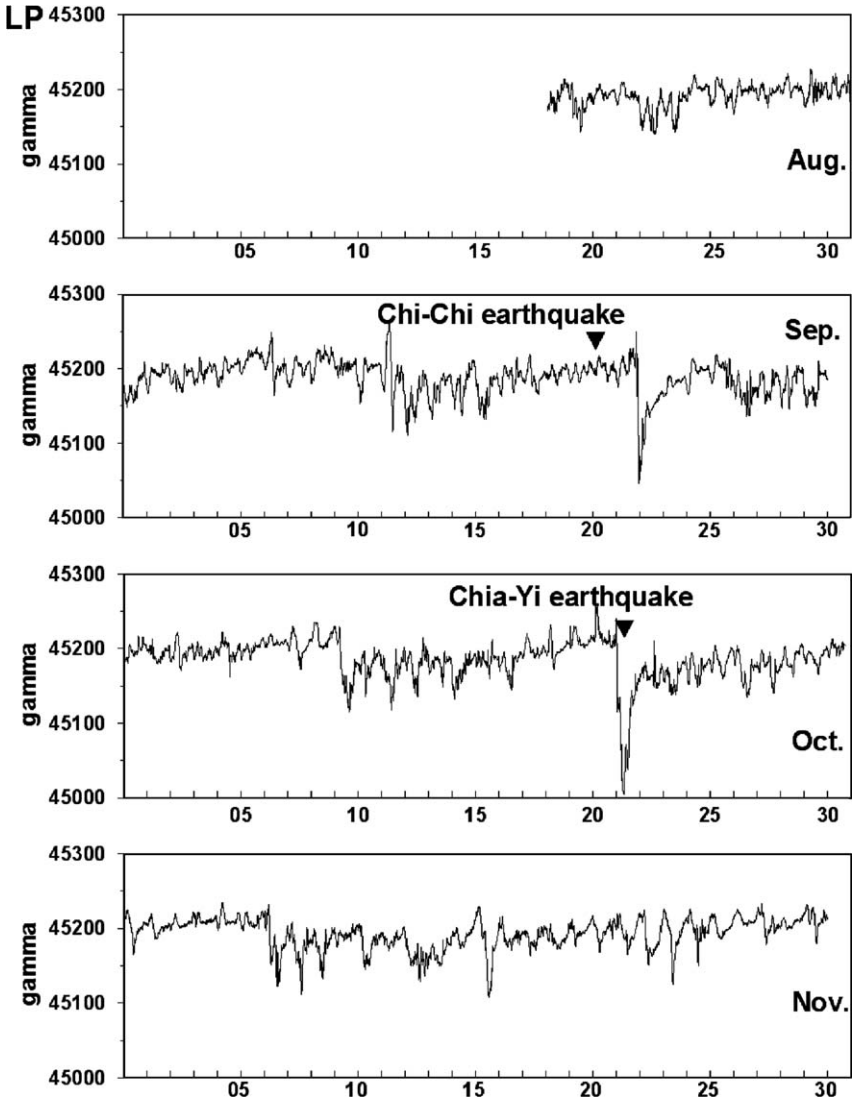


Fig. 6. Geomagnetic total intensity data recorded at the reference station (LP) from August to November 1999. No disturbance was observed before or after the Chi-Chi and Chia-Yi earthquakes, except for the two magnetic storms caused by an external source.

mainly occur near the southern end of the Chelungpu fault.

Scientists have observed anomalies appearing in ionospheric electron densities a few days before some strong earthquakes (Pulinets et al., 1998; Pulinets and Legen'ka, 1994; Liu et al., 2000, 2001). Liu et al. (2004a,b) examined measurements recorded by a local ionosonde and ground based receivers of the global positioning system (GPS) of in Taiwan during 1994–2003 (see Fig. 5). They find that the electron density at the F2-peak (NmF2) and the total electron content (TEC) of the GPS decrease significantly during 10:00–20:00 LT a few days prior to most of the $M \geqslant 6.0$ earthquakes in Taiwan. The recurrence interval of an $M \geqslant 5.0$ earthquake is about 13–15 days in Taiwan. To identify abnormal signals, we compute the median $\widetilde{X}$ of the previous 15-day TEC (or NmF2) and the associated inter-quartile range IQR, to construct the upper bound $\widetilde{X} + \mathrm{IQR}$ and lower bound $\widetilde{X} - \mathrm{IQR}$ at a certain local time (LT). Under the assumption of a normal distribution with mean $\mu$ and standard deviation $\sigma$ for the TEC (or NmF2), the expected value of $\widetilde{X}$ and IQR are $\mu$ and $1.34\sigma$, respectively (Klotz and Johnson, 1983). If an observed TEC (or NmF2) falls outside of either the associated lower or upper bound, we declare with a confidence level of about 80–85% that a lower or upper abnormal signal is detected.

Fig. 10a and b shows that the NmF2 and GPSTEC anomalously exceed the associated lower bound during 10:00–20:00 LT of 17 and 18 September 1999, which are 4 and 3 days before the Chi-Chi earthquake, respectively. The top and second rows in Fig. 11 further display the spatial precursors that the differential GPSTEC, which are the TEC subtracted from their medians, at 12:00, 14:00, and 16:00 LT on 17 and 18 September 1999, respectively. It can be seen that the GPSTEC of the two days significantly decreased around the Chi-Chi epicenter.

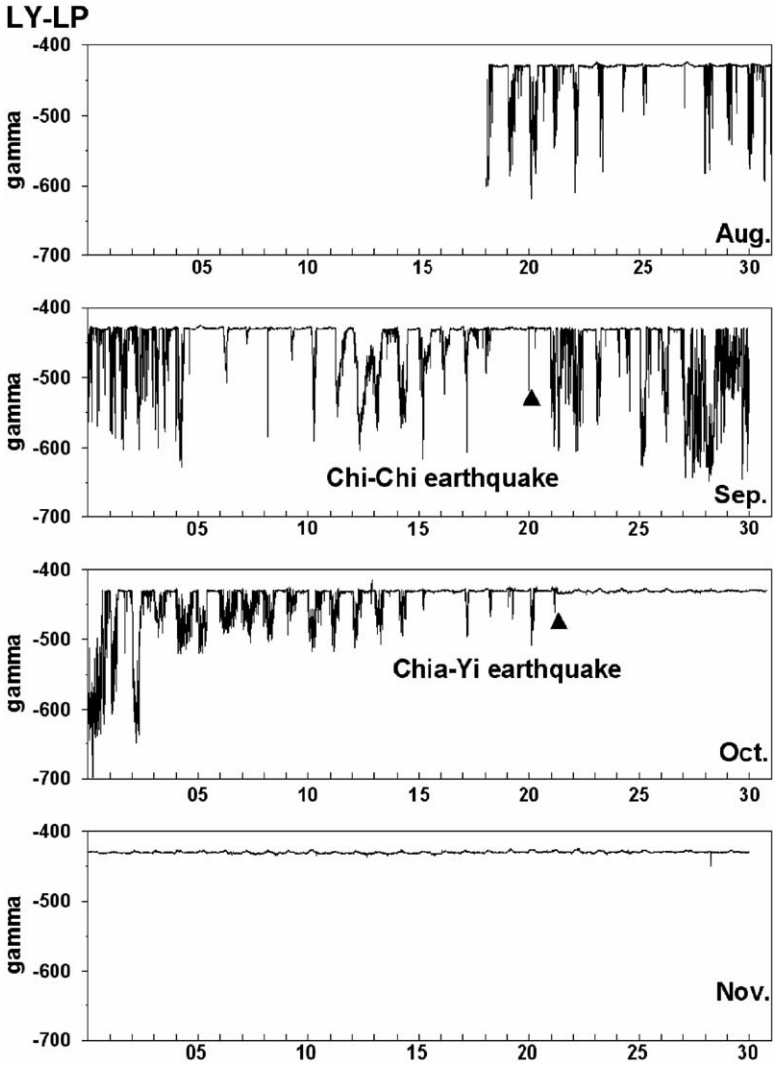


Fig. 7. Differences in geomagnetic total intensity between the Liyutan station (LY) and the reference station (LP). Geomagnetic fluctuations were clearly revealed. The largest amplitude was about 200 nTs. Large amplitude disturbances continued after the Chi-Chi earthquake. Following the Chia-Yi earthquake, geomagnetic fluctuations disappeared.

The coincidental occurrence in time of enhanced C–G lightenings and reduced ionospheric electron density appears to suggest a possible coupling mechanism between these two phenomena.

### *2.6. Stress changes for forecasting of aftershock distribution*

Advocates of static stress transfer argue that aftershocks often occur in regions that experienced an increase in Coulomb stress caused by the mainshock, and that earthquakes become less prevalent than before the mainshock in regions subject to a Coulomb stress drop (see reviews by Harris, 1998; Stein, 1999; King and Cocco, 2001). Most previous work related to this hypothesis has concentrated on strike-slip mainshocks, whose stress change does not vary greatly with depth. For thrust faulting, the stress change is depth-dependent (Lin and Stein, 2004), and thus the down-dip geometry and slip of the source fault, and the depth of aftershocks become essential to Coulomb stress analysis. The 20 September 1999 $M_w$ 7.6 Chi-Chi, Taiwan, earthquake on the Chelungpu fault is probably the world's best recorded major crutstal thrust event, with well determined spatial slip models derived from seismic, strong motion, and geodetic data. Equally important for this study, background seismicity and aftershock sequence are also recorded in unprecedented details, making it ideal for such investigation. A more complete description of this work can be found in Ma et al. (2005).

Using the detailed spatial slip distribution of the Chi-Chi earthquake source (Ji et al., 2003), we calculated the Coulomb stress changes following the method of Toda and Stein (2003). We then compared them with the seismicity rate changes derived from the 100-month seismic record centered on the mainshock. We place particular emphasis on the response of seismicity to the broad lobes of calculated stress increase (the trigger zones), and stress decrease

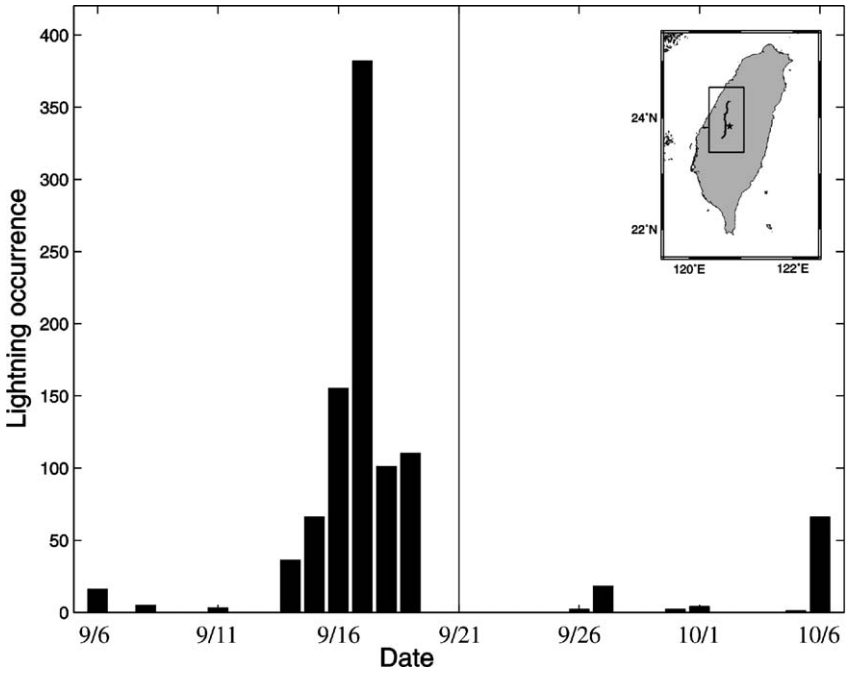


Fig. 8. Daily counts of cloud-to-ground lightnings along the Chelungpu fault from 6 September and 6 October 1999.

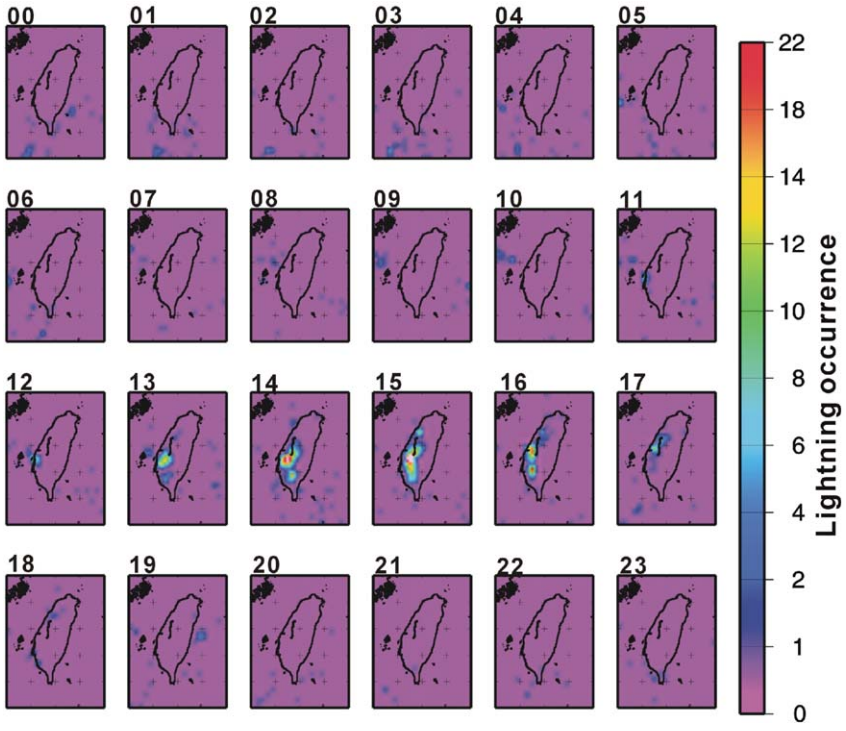


Fig. 9. Occurrence of cloud-to-ground lightnings at various local times of 17 September 1999.

(the stress shadows), and on whether the stress imparted to the aftershock rupture planes has indeed promoted their failure.

The Chi-Chi earthquake well exhibits the correlation between static Coulomb stress increases and aftershocks, and has thus far provided the strongest evidence that stress changes can promote seismicity. Several studies depend on the argument by resolving stress changes on aftershock focal mechanisms, which removes the assumption that the aftershocks are optimally oriented for failure. We compared the percentage of planes on which failure is promoted after the main shock relative to the percentage beforehand. We also examined the static stress triggering in observing predicted seismicity rate decreases in the stress

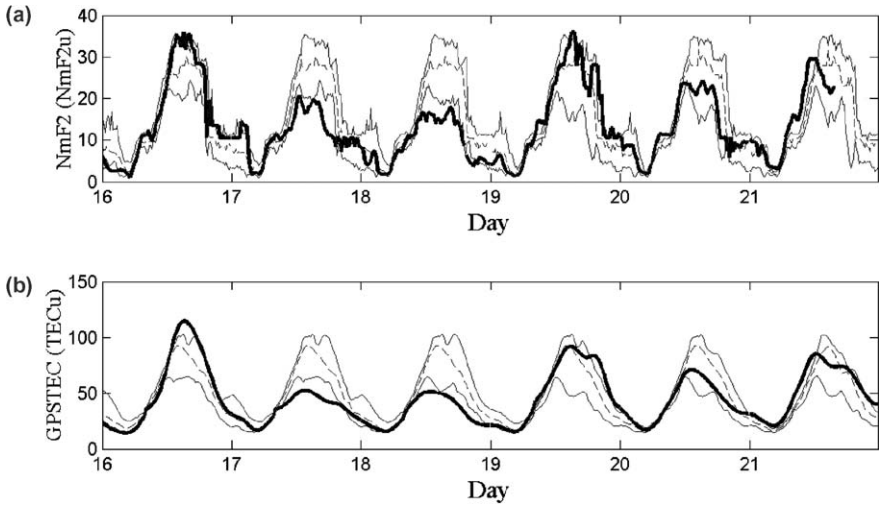


Fig. 10. Ionospheric anomalies observed during 16–21 September 1999. (a) Observation (dark curve) as well as the associated median (dashed curve) and upper/lower bounds (solid curves) of the NmF2. (b) Observation (dark curve) as well as the associated median (dashed curve) and upper/lower bounds (solid curves) of the GPSTEC.

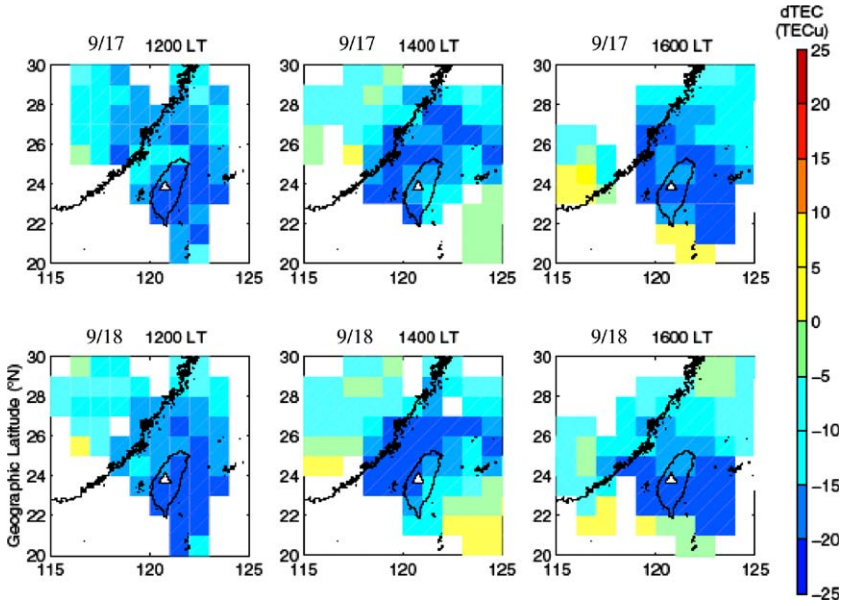


Fig. 11. Distribution of the GPSTEC decreases observed at 1200, 1400 and 1600 LT on 17 and 18 September 1999.

shadows, or sites of Coulomb stress decrease (Fig. 12). We find four lobes with statistically significant seismicity rate declines of 40–90% for 50 months, and they coincide with the stress shadows calculated for strike-slip faults, the dominant faulting mechanism. The rate drops are evident in uniform cell calculations, 100-month time series, and by visual inspection of the $M \geqslant 3$ seismicity.

When we shed the optimal orientation assumption and resolved stress changes on the nodal planes of the post-Chi-Chi shocks: 85% of the thrust and 65% of the strike-slip events receive calculated shear stress increases greater than 0.1 bar; this compares with 37% of the thrust and 49% of the strike-slip shocks during the pre-Chi-Chi period, for which no correlation would be expected (Fig. 13). To examine the Coulomb stress, which includes the role of unclamping in promoting failure, we measure the percentage increase after the Chi-Chi earthquake. Here we find a 26% increase in thrust events, and an 18% increase in strike-slip events receiving a Coulomb stress change greater than 0.1 bars. By comparison, Hardebeck et al. (1998) reported a 25% increase for Landers, Hardebeck and Hauksson (1999) reported a 20% increase for Northridge, and Seeber and Armbruster (2000) found a 30% increase for Landers (all three results are re-plotted in Fig. 5 of Stein, 1999).

Finally, no other mainshocks examined previously by Coulomb analysis has the Chi-Chi's abundance of large aftershocks; 7–9 out of 10 $M \geqslant 6$ shocks receive a positive

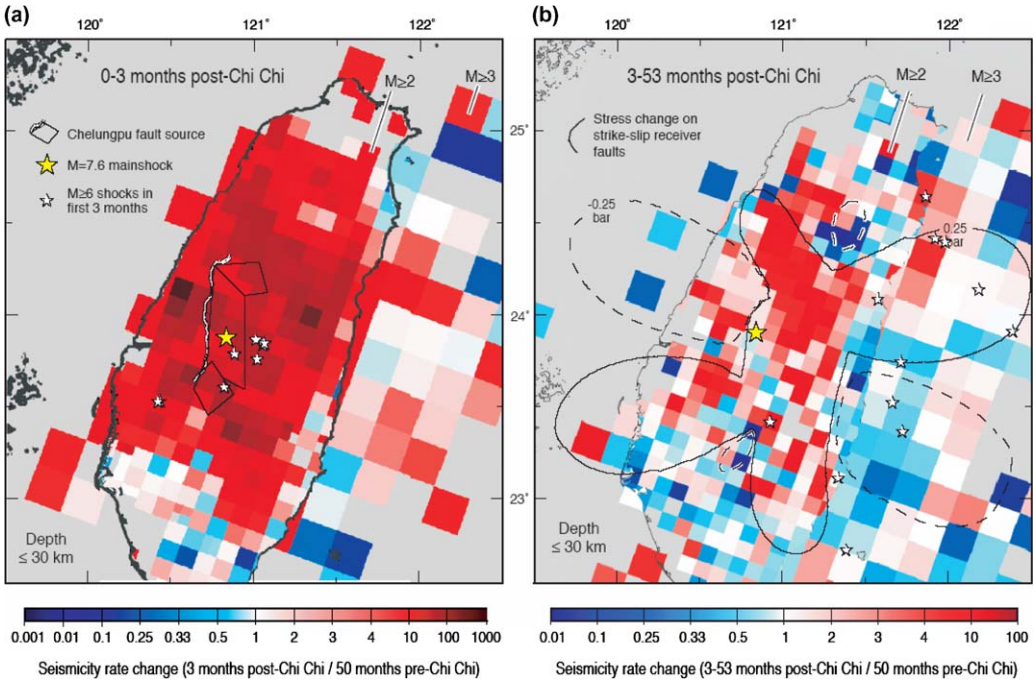


Fig. 12. Calculated seismicity rate change associated with the Chi-Chi earthquake. For the $10 \times 10 \times 30$ km cells within Taiwan, $M \geqslant 2$ shocks are used; for the $20 \times 20 \times 30$ km cells, $M \geqslant 3$ are used. (a) The first 3 months after the Chi-Chi earthquake are compared with the preceding 50 months. (b) Seismicity rate for the 50 months, starting 3 months after the Chi-Chi mainshock, are used; the modeled stress-change contours are from of Ma et al. (2005). Note that the seismicity-rate scale bars in (a) and (b) are different.

Coulomb stress change, with a mean stress increase of 4.4 bars. This study supports possible correlation of the occurrence of aftershocks to static stress changes of the mainshock. It, thus, provides a basis for forecasting the distribution of aftertshocks, which often can cause additional devastating damages after a large mainshock.

## 3. Discussion and conclusions

Under the iSTEP Program we have identified positively six types of precursory phenomena before the 1999 Chi-Chi earthquake. In terms of the dilatancy and diffusion model for earthquake preparation (Nur, 1972), the increase of P-wave travel-time, the surface deformation by DInSAR patterns, the *b*-value variations of earthquakes near the Chelungpu fault and the geomagnetic variations by the ZIZ method can be classified as long-term precursors, which may be explained by Stage II and III processes. On the other hand, the short-term geomagnetic variations, atmospheric and ionospheric anomalies are probably related to accelerate crustal instability just prior to the fault failure. They may be explained by the mechanism proposed by Freund (2003).

It has been well recognized that high *b*-values often appear before moderate or large earthquakes (Smith, 1981). Herein, we identify a significant increase of the *b*-value in 1997 near the west of northern Chelungpu fault. At the same time, however, we also observe a significant decrease of the *b*-value to the east of central Chelungpu fault. The anomalous increase and decrease of the *b*-values appearing around but in different directions of the Chelungpu fault suggest the fault is in an unstable environment for future rupture. Therefore, we confirm that the *b*-value anomaly appears about 2.5 years before the Chi-Chi earthquake. In fact, the location with anomalously increasing *b*-value is consistent with the findings in the P-wave travel-time residuals study and ground deformation patterns detected by InSAR. Moreover, the Chi-Chi epicenter is relatively close to an area with anomalously decreasing *b*-value where large earthquakes become more hazardous.

Chen et al. (2004) examined variation in the geomagnetic total field recorded by the eight stations in Taiwan from 1999 to 2001. They found a zero isoporic zone (ZIZ), which is defined as the annual change rate of geomagnetic parameters to be less than or equal to $\pm 5$ nT/yr appeared near the epicentral area about 2 years before the Chi-Chi earthquake. This generally agrees with the increase of the P-wave travel-time residuals, surface deformation, and the *b*-value changes which together appear to constitute as a group of long-term precursors. At this point, we still cannot find an obvious correlation between the shorter-term geomagnetic anomalies occurred about 2 months before (Akinaga et al., 2001; Yen et al., 2004; Liu et al., 2006) and the atmospheric/ionospheric anomalies occurred 3–4 days prior to (Liu et al., 2000, 2001) the Chi-Chi earthquake.

By contrast, it is interesting to note that the C–G lightning occurrences and GPSTEC significantly increase and decrease, respectively, 4 days before the Chi-Chi earthquake. This coincidence seems to imply that the

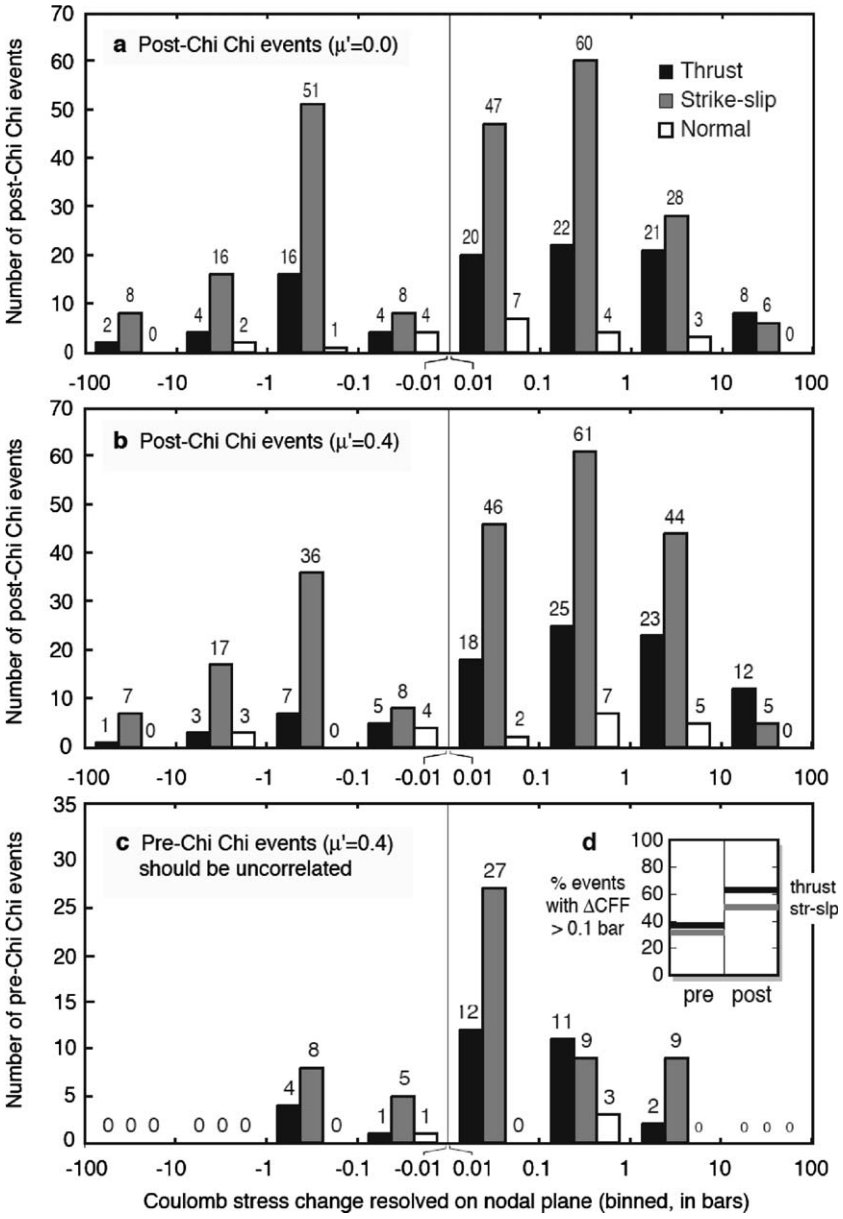


Fig. 13. Stress change on nodal planes for all events with known focal mechanisms. (a) Shear stress change on post-Chi-Chi nodal planes. (b) Coulomb stress change. For earthquakes with positive ΔCFF values on either nodal plane, the smaller of the two is chosen. For the earthquakes for which only one nodal plane has a positive ΔCFF, the positive one is chosen. For the events with negative ΔCFF on both nodal planes, the smaller absolute value is chosen. (c) Coulomb stress change calculated in the same manner for the pre-Chi-Chi focal mechanisms, which serves as a control sample. (d) The percentage of nodal planes with a calculated Coulomb stress change greater than 0.1 bars for the pre- and post-Chi-Chi periods, showing an increase following the Chi-Chi mainshock.

atmospheric and ionospheric anomalies to be electromagnetic coupled.

## References

Akinaga, Y., Hayakawa, M., Liu, J.Y., Yumoto, K., Hattori, K., 2001. A precursory ULF signature for the Chi-Chi earthquake in Taiwan. Natural Hazards Earth Syst. Sci. 1, 33–36.

Chen, C.H., Liu, J.Y., Yen, H.Y., Zeng, X., Yeh, Y.H., 2004. Changes of geomagnetic total field and occurrences of earthquakes in Taiwan. Terr. Atmos. Ocean. Sci. 15, 361–370.

Freund, F.T., 2003. Rocks that crackle and sparkle and glow: strange pre-earthquake phenomena. J. Sci. Explor. 17, 37–71.

Gutenberg, B., Richter, C.F., 1944. Frequency of earthquakes in California. Bull. Seism. Soc. Am. 34, 185–188.

Hardebeck, J.L., Hauksson, E., 1999. Background stress state plays a role in earthquake triggering. Eos. Trans. AGU 80 (46), 1005 (Fall Meet. Suppl.).

Hardebeck, J.L., Nazareth, J.J., Hauksson, E., 1998. The static stress change triggering model: constraints from two southern California aftershocks sequences. J. Geophys. Res. 103, 24,427–24,437.

Harris, R.A., 1998. Introduction to special section: stress triggers, stress shadows, and implication for seismic hazard. J. Geophys. Res. 103, 24,347–24,358.

Hayakawa, M. (Ed.), 1999. Atmospheric and Ionospheric Electromagnetic Phenomena Associated with Earthquakes. TERRAPUB, Tokyo, p. 997.

Hayakawa, M. 2000. Seismo Electromagnetics, Monograph of International Workshop on Seismo Electromagnetics, Tokyo.

Hayakawa, M., Fujinawa, Y. (Eds.), 1994. Electromagnetic Phenomena Related to Earthquake Prediction. TERRAPUB, Tokyo.

Hayakawa, M., Molchanov, O.A. (Eds.), 2002. Seismo-Electromagnetics: Lithosphere-Atmosphere-Ionosphere Coupling. TERRAPUB, Tokyo, p. 477.

Ji, C., Helmerger, D.V., Wald, D.J., Ma, K.F., 2003. Slip history and dynamic implications of the 1999 Chi-Chi, Taiwan, earthquake. J. Geophys. Res. 10 (B9), 2412. doi:10.1029/2002JB001764.

King, G.C.P., Cocco, M., 2001. Fault interaction by elastic stress changes: new clues from earthquake sequences. Adv. Geophys. 44, 1–28.

Klotz, S., Johnson, N.L., 1983. Encyclopedia of Statistical Sciences. John Wiley, Hoboken, NJ.

Lee, C.P., Tsai, Y.B., 2004. Variations of P-wave travel-time residuals before and after the 1999 Chi-Chi, Taiwan, earthquake. Bull. Seism. Soc. Am. 94, 2348–2365.

Lin, J., Stein, R.S., 2004. Stress triggering in thrust and subduction earthquakes, and stress interaction between the southern San Andreas and nearby thrust and strike-slip faults. J. Geophys. Res. 109, B02303. doi:10.1029/2003JB002607.

Liu, J.Y., Chen, Y.I., Pulinets, S.A., Tsai, Y.B., Chuo, Y.J., 2000. Seismo-ionospheric signatures prior to $M \geqslant 6.0$ Taiwan earthquakes. Geophys. Res. Lett. 27, 3113–3116.

Liu, J.Y., Chen, Y.I., Chuo, Y.J., Tsai, H.F., 2001. Variations of ionospheric total electron content during the Chi-Chi earthquake. Geophys. Res. Lett. 28, 1383–1386.

Liu, J.Y., Chuo, Y.J., Shan, S.J., Tsai, Y.B., Chen, Y.I., Pulinets, S.A., Yu, S.B., 2004a. Pre-earthquake ionospheric anomalies registered by continuous GPS TEC measurements. Ann. Geophys. 22, 1585–1593.

Liu, J.Y., Chen, Y.I., Jhuang, H.K., Lin, Y.H., 2004b. Ionospheric foF2 and TEC anomalous days associated with $M \geqslant 5.0$ earthquakes in Taiwan during 1997–1999. Terr. Atmos. Ocean. Sci. 15, 371–383.

Liu, J.Y., Chen, C.H., Chen, Y.I., Yen, H.Y., Hattori, K., Yumoto, K., 2006. Seismo-geomagnetic anomalies and $M \geqslant 5.0$ earthquakes observed in Taiwan during 1988–2001. Phys. Chem. Earth. 31 (4–9), 215–222.

Ma, K.F., Chan, C.H., Stein, R.S., 2005. Response of seismicity to Coulomb stress triggers and shadows of the 1999 $M_w = 7.6$ Chi-Chi, Taiwan, earthquake. J. Geophys. Res. 110, B05S19. doi:10.1029/2004JB003389.

Nur, A., 1972. Dilatancy, pore fluids, and premonitory variations of $t_s/t_p$ travel times. Bull. Seism. Soc. Am. 62, 1217–1222.

Pulinets, S.A., Legen'ka, A.D., 1994. Pre-earthquakes effects and their possible mechanisms. In: Dusty and Dirty PlasmasNoise and Chaos in Space and in the Laboratory. Plenum Publishing, New York, pp. 545–557.

Pulinets, S.A., Khegai, V.V., Boyarchuk, K.A., Lomonosov, A.M., 1998. Atomspheric electric field as a source of ionospheric variability. Physics-Uspekhi 41, 515–522.

Seeber, L., Armbruster, J.G., 2000. Earthquakes as beacons of stress change. Nature 407, 69–72.

Shi, Y., Bolt, B.A., 1982. The standard error of the magnitude–frequency $b$ value. Bull. Seism. Soc. Am. 72, 1677–1687.

Smith, W.D., 1981. The $b$-value as an earthquake precursor. Nature 289, 136–139.

Stein, R.S., 1999. The role of stress transfer in earthquake occurrence. Nature 402, 605–609.

Toda, S., Stein, R.S., 2003. Toggling of seismicity by the 1997 Kagoshima earthquake couplet: a demonstration of time-dependent stress transfer. J. Geophys. Res. 109, B02303. doi:10.1029/2003JB002527.

Wiemer, S., Katsumata, K., 1999. Spatial variability of seismicity parameters in aftershock zones. J. Geophys. Res. 104, 13,135–13,151.

Yen, H.Y., Chen, C.H., Yeh, Y.H., Liu, J.Y., Lin, C.R., Tsai, Y.B., 2004. Geomagnetic fluctuations during the 1999 Chi-Chi earthquakes in Taiwan. Earth Planets Space 56, 39–45.